Journal of Power Sources 319 (2016) 210–218

Contents lists available at ScienceDirect

Journal of Power Sources

journal homepage: www.elsevier.com/locate/jpowsour

Carbon-shell-decorated *p*-semiconductor $PbMoO_4$ nanocrystals for efficient and stable photocathode of photoelectrochemical water reduction

Ligang Wang, Hanqin Tang, Yang Tian[*]

Department of Chemistry, Beijing Key Laboratory for Optical Materials and Photonic Devices, Capital Normal University, Haidian District, Beijing, 100048, China

HIGHLIGHTS

- $PbMoO_4$ nanocrystals coated with C shell were facilely controlled to fabricate.
- 2-nm carbon shell coated $PbMoO_4$ generated superior photoelectrochemical properties.
- The charge transfer efficiency of photoelectrochemical was increased 7.4%.
- The charge separation efficiency of photoelectrochemical was 56% enhanced.
- The photoelectrochemical stability was enhanced greatly.

GRAPHICAL ABSTRACT

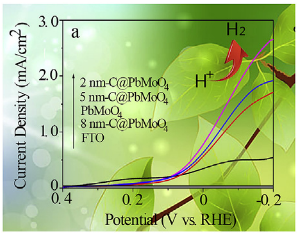

ARTICLE INFO

Article history:
Received 12 November 2015
Received in revised form
10 April 2016
Accepted 11 April 2016
Available online 19 April 2016

Keywords:
$PbMoO_4$
Photoelectrochemical
Water splitting
Photocathode
Carbon shell

ABSTRACT

Photoelectrochemical (PEC) water splitting using semiconductors is a promising method for the future scalable production of renewable hydrogen fuels. The critical issues in PEC water splitting include the development of the photoelectrode materials with high efficiency and long-term stability, especially for p-type semiconductor photocathodes. Herein, we report the use of citric acid (CA) pyrolysis to prepare carbon-shell-decorated $PbMoO_4$ (C@$PbMoO_4$) nanocrystals via a simple solvothermal method. Different carbon shell thicknesses below 10 nm were generated by varying the amount of CA in the precursor solution. In contrast, without using CA, bare $PbMoO_4$ nanocrystals were obtained. The PEC experiments showed that 2-nm carbon shell could preferably improve the water splitting performance of $PbMoO_4$: the photocurrent density of 2-nm C@$PbMoO_4$ is nearly 2-fold high as that of bare $PbMoO_4$ at 0 V versus reversible hydrogen electrode (RHE). The surface charge transfer efficiency of 2-nm C@$PbMoO_4$ in the PEC process was tested to increase from 83% to 90.4%, the charge separation efficiency enhanced 56%, and the PEC stability also greatly increased compared to those of the bare $PbMoO_4$ nanocrystals. This strategy could be applied to other p-type semiconducting photocathodes for low-cost solar-fuel-generation devices.

1. Introduction

Hydrogen is a clean and promising sustainable alternative to

---

[*] Corresponding author.
E-mail address: tianyang@cnu.edu.cn (Y. Tian).

http://dx.doi.org/10.1016/j.jpowsour.2016.04.059
0378-7753/

fossil fuels to meet the global energy demands. With hydrogen fuel as an environmentally and friendly alternative, photoelectrochemical (PEC) water splitting with semiconductor electrode materials has become a suitable option ever since the report of the Honda-Fujishima effect [1–6]. In contrast to photocatalyst hydrogen generation, PEC water splitting can be achieved through the application of some external bias, even if powdered photocatalysts do not possess energy-band potentials that are suitable for water splitting [7]. The use of advanced metal oxide and sulfide semiconductors as active photoelectrode materials for PEC cells has been studied widely. However, it remains challenges to develop new semiconductor photoelectrode materials with low cost, high efficiency, and good stability for hydrogen generation via solar energy. In particular, most p-type semiconductor materials are generally unstable when used as photocathodes for proton reduction in an aqueous environment. This phenomenon has been explained using thermodynamics, as the conduction band potential is more negative than the reduction potential of the metal ions in the lattice, leading to the reductive decomposition of the semiconductor surface and the loss of photoactivity [8].

Based on these concerns, an investigation targeting core-shell nanostructures for enhancing PEC stability and efficiency might provide an alternative route to engineer semiconductor materials. For example, the p-semiconductor Si is often coated with a corrosion-resistant layer, such as TiO_2, WO_3, SnO_2, Fe_2O_3, etc., to enhance the stability for the PEC evolution of H_2 [9–12]. Additionally, many n-semiconductors were also reported to be coated with various shells, such as ZnO/CdTe core-shell nanocables [13], Fe_2O_3/ZnO core-shell nanowires [14], TiO_2/FeOOH nanorods [15,16], and WO_3/$BiVO_4$ core-shell nanowires [17], to improve PEC water splitting performances. However, the shell compositions of all the above examples are semiconductor materials with poor conductivity, hindering the transfer of charge carriers at a certain level. As a good conductor, carbon has often been used as shell-coating material on electrodes for the applications in such as Li ions batteries [18–20], supercapacitor [21], electrocatalysis [22], and solar cells [23]. To the best of our knowledge, there are few reports on carbon-coated semiconductor nanocrystals as photoelectrode materials to improve the stability and efficiency of PEC water splitting.

As a p-type semiconductor, lead molybdate ($PbMoO_4$) has gained increasing interest due to its potential applications in the fields such as photoluminescence, solid-state lasers, scintillating materials, humidity sensors, and photocatalysts [24–27]. Moreover, $PbMoO_4$ crystals can be found in the natural form of an abundant mineral called "Wulfenite". $PbMoO_4$ crystals in a tetragonal scheelite structure have point group symmetry 4/m and space group *I41/a*, with two formula units per primitive cell [28,29]. Each Mo atom is surrounded by four equivalent O atoms composed of $[MoO_4]^{2-}$ tetrahedrons, which are linked via Pb^{2+}. The semiconductor properties of $PbMoO_4$ arise due to the interactions between the Mo d states and O 2p orbitals, which have some covalent contribution to the ionic bonds. The value of the band gap as determined experimentally lies between 3.1 and 3.4 eV, whereas calculations give a much wider energy range, i.e., from 2.6 eV to 4.8 eV [24,26,30,31]. In the past decades, although many efforts have been devoted to $PbMoO_4$ semiconductor preparation, few of them are concerned on the use in PEC water splitting [32–35].

In this work, we report the preparation of carbon shell coating on $PbMoO_4$ nanocrystals (C@$PbMoO_4$) via a simple solvothermal method with citric acid (CA) as the C source. The thickness of the carbon shell was controlled facilely to 2 nm, 5 nm, and 8 nm by varying the amount of CA in the precursor solution. The prepared C@$PbMoO_4$ nanocrystals were investigated as photocathode materials for PEC water splitting. The C@$PbMoO_4$ with the carbon shell in 2-nm thickness generated the most remarkable PEC photocurrent density than did bare $PbMoO_4$, as well as the 5-nm C@$PbMoO_4$ and 8-nm C@$PbMoO_4$ samples. The surface charge transfer efficiency of 2-nm C@ $PbMoO_4$ in PEC water splitting were tested to increase by 7.4% (from 83% to 90.4%), the charge separation efficiency enhanced 56%, and the PEC stability increased greatly compared to those of bare $PbMoO_4$ nanocrystals.

2. Experimental section

2.1. Chemicals

Lead acetate trihydrate ($PbAc_2 \cdot 3H_2O$, 99%) was purchased from Tianjin Guangfu Co., Ltd. Ammonium molybdate tetrahydrate ($(NH_4)_6Mo_7O_{24} \cdot 4H_2O$, 99% mass fraction) was obtained from Shenyang reagent factory. Citric acid (CA, 99%) was obtained from Beijing chemical factory. Fluorine-doped tin oxide (FTO) coated glass was provided by Tianjin IDA Co., Ltd. Deionized water was used as the solvent in solvothermal synthesis and electrochemical experiments. All chemicals were used as received without further purification.

2.2. Synthesis of 2-nm, 5-nm and 8-nm C@$PbMoO_4$ nanocrystals and bare $PbMoO_4$ nanocrystals

In a typical procedure to prepare 2-nm C@$PbMoO_4$ nanocrystals, $PbAc_2 \cdot 3H_2O$ (0.0759 g, 0.2 mmol), $(NH_4)_6Mo_7O_{24} \cdot 4H_2O$ (0.0353 g, 0.028 mmol) and citric acid (0.0210 g, 0.5 mmol) were added to 12.0 mL deionized water in a Teflon-lined stainless steel autoclave with a capacity of 20.0 mL at room temperature, and stirred for 10 min. After the autoclave was sealed and maintained at 200 °C for 1 h in a preheated oven, it was taken out and cooled to room temperature naturally. White products were collected after being repeatedly washed with deionized water and anhydrous ethanol, and then dried in a vacuum oven. Then the obtained sample was redispersed in deionized water (~5 mL) and stored for their posterior use.

5-nm and 8-nm C@$PbMoO_4$ nanocrystals were prepared via a similar method with 2-nm C@$PbMoO_4$ nanocrystals, but added 0.0420 g and 0.210 g citric acid into the precursor solution, respectively.

Bare $PbMoO_4$ nanocrystals were prepared via a similar method with 2-nm C@$PbMoO_4$ nanocrystals, without adding citric acid into the precursor solution.

2.3. Characterization

Powder X-ray diffraction (XRD) patterns were collected on a Rigaku D/Max 2200 PC diffractometer with Cu Ka radiation ($\lambda = 1.5418$ Å) and a graphite monochromator from 10° to 80° with a scanning rate of 5.0° per min. Unit cell dimensions and the crystallinity were determined using the JADE 5 program for X-ray diffraction pattern processing, identification, and quantification. The size and morphology of the obtained samples were characterized on a transmission electron microscope (TEM, JEM100-CXII) equipped with a selected area electron diffractometer (SAED). The structure and lattice fringes of nanocrystals were observed by using a high resolution TEM (HRTEM, FEI Tecnai G2 F30) equipped with a scanning transmission electron microscope (STEM). The chemical composition of the as-prepared $PbMoO_4$ and C@$PbMoO_4$ nanocrystals were analyzed by energy dispersive X-ray spectroscopy (EDX, Oxford). To gain a better understanding of the elemental distribution throughout these nanocrystals, the samples were characterized using high angle annular dark field-scanning TEM (HAADF-STEM) imaging in conjunction with EDX mapping. Thermogravimetric analysis (TGA, NETZSCH STA 449F3) was carried out